# Investigation of the Bohr-Independence Hypothesis for Nuclear Reactions in the Continuum: $\alpha+Co^{59}$, $p+Ni^{62}$ and $\alpha+Fe^{56}$, $p+Cl^{59}$†

M. J. Fluss,*‡ J. M. Miller, J. M. D'Auria,§ N. Dudey,‡ B. M. Foreman, Jr.,‖ L. Kowalski, and R. C. Reedy
*Chemistry Department, Columbia University, New York, New York 10027*

(Received 13 March 1969)

Measurements were made of the energy spectra at various angles of protons and $\alpha$ particles emitted from the reactions of protons with $Ni^{62}$ and $\alpha$ particles with $Co^{59}$ to determine the extent to which the deexcitation of the reaction intermediate, $Cu^{63}$ at 20.2-MeV excitation energy, is independent of its mode of formation. Similarly, the reaction intermediate $Ni^{60}$ at 23.6 MeV was formed by protons on $Co^{59}$ and $\alpha$ particles on $Fe^{56}$, again to determine to what degree its deexcitation by proton and $\alpha$-particle emission is independent of its mode of formation. Small differences in the shapes of corresponding energy spectra [$(p, p')$ versus $(\alpha, p)$, and $(\alpha, \alpha')$ versus $(p, \alpha)$] that were observed in apparent violation of the Bohr-independence hypothesis are removed after account has been taken of the effects of angular-momentum conservation. The observed enhancement of the ratio of cross sections $\sigma(x, p)/\sigma(x, \alpha)$ for the proton entrance channel over that for the $\alpha$ entrance channel cannot be interpreted in terms of angular-momentum conservation. The consequences of the possibility of isotopic-spin conservation, when considered, lead to enhanced proton reemission similar to that observed experimentally.

## INTRODUCTION

In 1936, Bohr[1] suggested the compound-nucleus mechanism for nuclear reactions. Invoking the statistical assumption extends the Bohr model to the region of overlapping levels. Inherent to this description of the compound-nucleus mechanism is the concept of complete independence of the entrance and exit channels. The only "memory" that the system maintains is that of the "constants of the motion": momentum, angular momentum, nucleon number, parity, energy, and possibly, isotopic spin. "The particular channel that served as the entrance channel has been forgotten.[2]" Thus, what may be called the independence hypothesis is a general feature of the compound-nucleus mechanism that was proposed by Bohr.

Consider the compound nucleus $C$ at an excitation energy $E$ which can be formed by two corresponding reaction systems which can decay through at least two distinguishable exit channels. Such a system is illustrated by the diagram

$$a+A \quad d+D$$
$$\searrow \quad \nearrow$$
$$C \quad ,$$
$$\nearrow \quad \searrow$$
$$b+B \quad e+E$$

where $A$ and $B$ are the corresponding target nuclei, $a$ and $b$ the corresponding projectiles, $d$ and $e$ the emitted particles, and $D$ and $E$ the residual nuclei. Since the residual nuclei $D$ and $E$ need not be in their ground states, the particles $d$ and $e$ are each emitted with a spectrum of energies. Preferably, one would verify the independence hypothesis for such a system by observing the energy spectra of particles emitted from $C$ at several angles; that is, by measurement of the differential cross sections $d^2\sigma/d\Omega dE$. In previous experiments,[3–20] though, this was not done; the distinguishable exit channels were instead identified by those residual nuclei ($D$, $E$, etc.) which happened to be radioactive. Thus these previous experiments may be called integral experiments in the sense that the quantity that is measured is the integral of the differential cross sections for the emitted particles leading to a particular radioactive product.

In an integral experiment, the independence hypothesis demands that $\sigma(a, D)/\sigma(a, E)$ be equal to $\sigma(b, D)/\sigma(b, E)$, provided that the only constant of the motion which must be considered is the energy of the compound nucleus. The equality of these ratios of cross sections is

† Work supported in part by the U. S. Atomic Energy Commission.

* Submitted in partial fulfillment for the degree of Doctor of Philosophy at Columbia University.

‡ Present address: Argonne National Laboratory, Argonne, Ill.

§ Present address: Simon Fraser University, Vancouver, B. C., Canada.

‖ Present address: American Institute of Physics, New York, N. Y. 10027.

[1] N. Bohr, Nature **137**, 344 (1936).

[2] J. Blatt and V. F. Weisskopf, *Theoretical Nuclear Physics* (John Wiley & Sons, Inc., New York, 1952).

[3] S. N. Ghoshal, Phys. Rev. **80**, 939 (1950).

[4] C. F. Smith, Jr., University of California Radiation Laboratory Report No. UCRL-1182, 1965 (unpublished).

[5] S. Tanaka, J. Phys. Soc. Japan **15**, 2159 (1960).

[6] J. W. Meadows, Phys. Rev. **91**, 885 (1953).

[7] F. K. McGowan, P. H. Stelson, and W. G. Smith, Bull. Am. Phys. Soc. **5**, 266 (1960).

[8] H. A. Howe, Phys. Rev. **109**, 2083 (1960).

[9] J. P. Blaser, F. Boehm, P. Marmier, and D. C. Peaslee, Helv. Phys. Acta **24**, 3 (1951).

[10] B. L. Cohen and E. Newman, Phys. Rev. **99**, 718 (1955).

[11] C. M. Stearns, Report No., NYO-10387, 1962 (unpublished).

[12] J. R. Grover and R. J. Nagle, Phys. Rev. **134**, B1248 (1964).

[13] N. T. Porile, S. Tanaka, H. Amano, M. Furukawa, S. Iwata, and M. Yaki, Nucl. Phys. **43**, 500 (1963).

[14] W. John, Phys. Rev. **103**, 704 (1956).

[15] J. W. Meadows and R. B. Holt, Phys. Rev. **83**, 47 (1951).

[16] M. A. Tamers and R. Wolfgang, Phys. Rev. **117**, 812 (1960).

[17] B. L. Cohen, H. L. Reynolds, and A. Zucker, Phys. Rev. **96**, 1617 (1954).

[18] N. M. Hintz and N. F. Ramsey, Phys. Rev. **88**, 19 (1952).

[19] K. L. Chen and J. M. Miller, Phys. Rev. **134**, B1269 (1964).

[20] S. Tanaka, M. Furukawa, S. Iwata, M. Yaki, H. Amano, and T. Mikumo, J. Phys. Soc. Japan **15**, 2125 (1960).

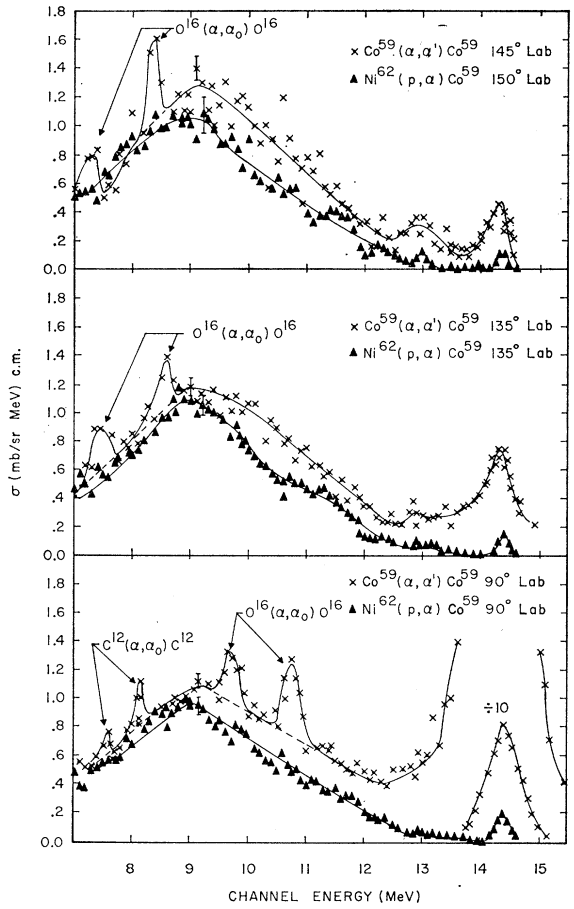


FIG. 1. Typical energy spectra for the reactions $Co^{59}(\alpha, \alpha')Co^{59}$ and $Ni^{62}(p, \alpha)Co^{59}$. The dashed-line part of the spectrum represents the estimated spectrum after correction is made for the indicated impurities.

then taken to be an experimental verification of the Bohr-independence hypothesis.

The first integral test of the independence hypothesis was carried out by Ghoshal[3], who compared the behavior of the $Zn^{64}$ compound nucleus formed by $p+Cu^{63}$ and by $\alpha+N^{60}$. Comparisons were made of the excitation functions of the $(x, n)$, $(x, 2n)$, and $(x, pn)$ reactions, where $x$ is either a proton or $\alpha$ particle. Verification of the independence hypothesis was obtained in Ghoshal's work by observing that the ratio of cross sections $\sigma(x, pn)/\sigma(x, 2n)$ is independent of the projectile $x$, which was used to form the compound nucleus over most of the region of excitation energy that was studied. Other investigations of this same system[4,10] have essentially validated Ghoshal's results. In one of these experiments though, the one by Smith,[4] the $He^3+Ni^{61}$ and $C^{12}+Cr^{52}$ reactions were also investigated in what thereby became a four-way "Ghoshal experiment." While Smith also found that the proton and $\alpha$-particle entrance channel possibly conformed to the requirement of independence, those for the $He^3$ and $C^{12}$ did not. In some studies of other compound systems, there have also been significant apparent violations of the independence hypothesis.

For those results in which an apparent violation of independence is observed, two questions should be asked:

(a) Are all of the constants of the motion other than energy the same in the corresponding entrance channels, and if not, is this fact of significance to the ratios of observed cross sections?

(b) Is the general behavior of the cross section for each reaction under investigation characteristic of that expected for compound-nucleus reactions?

The investigation by Grover and Nagle[12] of the ratios of cross sections for the corresponding pairs of reactions—$Bi^{209}(p, n)Po^{209}$, $Bi^{209}(p, 2n)Po^{208}$, and $Pb^{206}(\alpha, n)Po^{209}$, $Pb^{206}(\alpha, 2n)Po^{209}$—near the threshold for the two-neutron-out reactions, showed the decisive role that angular momentum conservation can play in producing an apparent violation of the independence hypothesis when the angular momenta distributions are not the same in corresponding entrance channels. The divergences found in other systems, though,[4–11] could not be so readily interpreted. Often these divergences

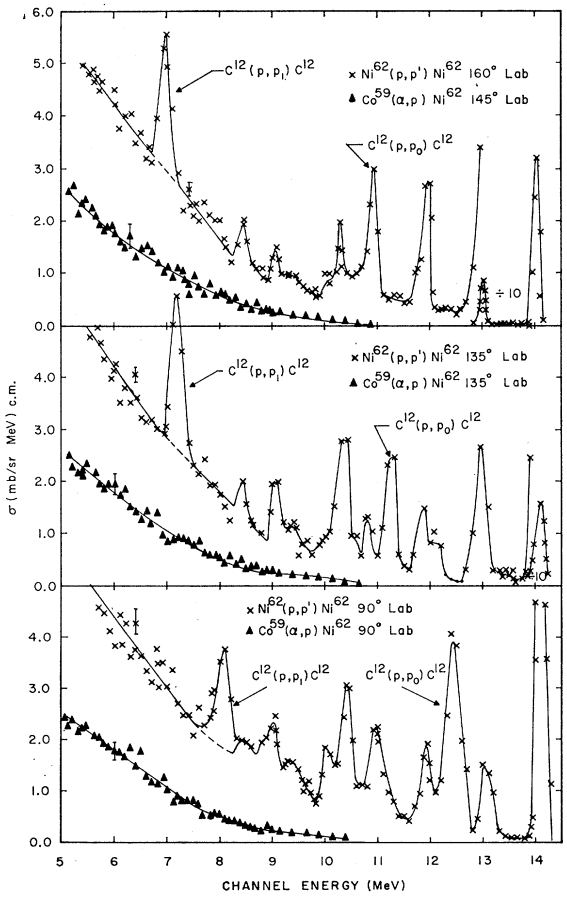


FIG. 2. Typical energy spectra for the reactions $Co^{59}(\alpha, p)Ni^{62}$ and $Ni^{62}(p, p')Ni^{62}$. See Fig. 1 for explanation of the dashed line.

TABLE I. The c.m. cross sections are in units of mb/sr for intervals of 1-MeV channel energy. They are estimated to be accurate to ±10%.

| Energy interval $\theta_{lab}$ (deg) | Cross sections in 1-MeV intervals in mb/sr $Co^{59}(\alpha, p)N^{62}$ 6–7 | 7–8 | 8–9 | 9–10 | $N^{62}(p, p')N^{62}$ 6–7 | 7–8 | 8–9 | 9–10 |
|---|---|---|---|---|---|---|---|---|
| 35.8 | 1.73 | 0.63 | 0.36 | 0.174 | | | | |
| 45 | 1.33 | 0.76 | 0.52 | 0.24 | 7.69 | 6.70 | 3.27 | 3.74 |
| 60 | 1.46 | 0.85 | 0.42 | 0.21 | 3.76 | 3.11 | 3.32 | 1.91 |
| 75 | 1.30 | 0.73 | 0.31 | 0.16 | 3.41 | 2.56 | 1.97 | 1.89 |
| 90 | 1.39 | 0.74 | 0.37 | 0.18 | 3.31 | 2.40 | 1.80 | 1.36 |
| 100 | | | | | 3.64 | 2.48 | 1.79 | 1.30 |
| 110 | | | | | 3.50 | 2.42 | 1.60 | 1.18 |
| 120 | 1.36 | 0.76 | 0.36 | 0.18 | 3.52 | 2.55 | 1.49 | 1.14 |
| 135 | 1.34 | 0.75 | 0.36 | 0.18 | 3.51 | 2.43 | 1.38 | 1.01 |
| 145 | 1.45 | 0.84 | 0.38 | 0.20 | 3.53 | 2.44 | 1.35 | 0.96 |
| 160 | | | | | 3.61 | 2.36 | 1.35 | 0.903 |

take the following form: Plots of corresponding ratios of reaction cross sections against excitation energy of the compound nucleus give curves that are congruent over a substantial range of excitation energy, but can only be brought into coincidence by a linear translation either along the cross-section–ratio axis or along the excitation-energy axis.

It has been suggested[4,11,13] that, at a certain level of approximation, the displacement along the excitation-energy axis implies that the apparent violation of independence is caused by a mismatch of angular momentum distributions in the two corresponding entrance channels. Grover and Nagle[12] showed that such a mismatch, while important, does not cause a simple linear shift. On the other hand, a displacement along the vertical axis, the cross-section–ratio axis, of the congruent ratio curves carried the interesting implication that while there may be relative enhancement of certain exit channels depending on the entrance channel, the energy spectra of the particles in all the various corresponding exit channels have essentially the same shape. This implication was one of the main motivations for the present work, in which measurements were made of the corresponding energy and angular distributions of emitted particles from corresponding reactions.

In addition, measurements of the spectra of emitted particles afford a better opportunity for the identification of compound-nuclear events. Since all of the previous experiments were of the integral type, the only criterion available to establish the compound nature of the observed exit channels is the shape of the excitation function for the radioactive product formed in each of the measurable exit channels. The excitation function for a compound-nucleus reaction is characterized by a rapid increase in the cross section with energy as the threshold energy for that particular reaction is exceeded; this is followed by a broad maximum which lasts until other competing reactions begin to dominate as their threshold energies are passed, and the cross section for the reaction of interest then decreases rapidly with increasing energy. An unexpectedly slowly decreasing cross section for a particular product is often taken as evidence for other than compound-nuclear reactions. Thus, to minimize contributions from non compound-nuclear events, it is preferable to compare corresponding excitation functions in the vicinity of their maxima.

With energy spectra, on the other hand, there are two criteria available: the energy spectrum at a given angle of emission and the angular distribution of the particles emitted within a given energy interval. Thus, it is rather simple to see if the shapes of energy spectra

TABLE II. The c.m. cross sections are in units of mb/sr for intervals of 1-MeV channel energy. They are estimated to be accurate to ±10%.

| Energy interval $\theta_{lab}$ (deg) | Cross sections in 1-MeV intervals in mb/sr $Co^{59}(\alpha, \alpha)Co^{59}$ 7–8 | 8–9 | 9–10 | 10–11 | 11–12 | $Ni^{2}(p, \alpha)Co^{59}$ 7–8 | 8–9 | 9–10 | 10–11 | 11–12 |
|---|---|---|---|---|---|---|---|---|---|---|
| 30 | | | | | | 0.57 | 0.86 | 0.96 | 0.66 | 0.49 |
| 37 | | | | | | 0.53 | 0.90 | 0.91 | 0.67 | 0.46 |
| 45 | | | | | | 0.55 | 0.89 | 0.92 | 0.61 | 0.45 |
| 60 | 0.37 | 0.92 | 1.08 | 0.90 | 0.56 | 0.57 | 0.88 | 0.88 | 0.57 | 0.42 |
| 75 | 0.35 | 0.88 | 1.01 | 0.84 | 0.48 | 0.52 | 0.86 | 0.88 | 0.58 | 0.33 |
| 90 | 0.31 | 0.72 | 0.89 | 0.68 | 0.42 | 0.53 | 0.86 | 0.85 | 0.54 | 0.33 |
| 105 | | | | | | 0.58 | 0.86 | 0.85 | 0.53 | 0.32 |
| 120 | 0.39 | 0.84 | 0.97 | 0.71 | 0.49 | 0.57 | 0.87 | 0.83 | 0.54 | 0.33 |
| 135 | 0.44 | 0.91 | 1.05 | 0.81 | 0.47 | 0.62 | 0.95 | 0.89 | 0.58 | 0.33 |
| 145 | 0.43 | 0.85 | 1.11 | 0.88 | 0.52 | | | | | |
| 150 | | | | | | 0.62 | 0.97 | 0.95 | 0.58 | 0.41 |

TABLE III. The c.m. cross sections are in units of mb/sr for intervals of 1-MeV channel energy. They are estimated to be accurate to ±10%.

| Energy interval $\theta_{lab}$ (deg) | Cross sections in 1-MeV intervals in mb/sr $Fe^{56}(\alpha,\alpha)Fe^{56}$ 7–8 | 8–9 | 9–10 | 10–11 | 11–12 | $Co^{59}(p,\alpha)Fe^{56}$ 7–8 | 8–9 | 9–10 | 10–11 | 11–12 |
|---|---|---|---|---|---|---|---|---|---|---|
| 45 | | | | | | 0.77 | 1.27 | 1.09 | 0.86 | 0.61 |
| 60 | 0.88 | 1.49 | 1.50 | 1.20 | 1.05 | | | | | |
| 68 | | | | | | 0.79 | 1.08 | 1.11 | 0.74 | 0.45 |
| 75 | 1.02 | 1.39 | 1.47 | 1.17 | 0.91 | | | | | |
| 90 | 0.96 | 1.38 | 1.23 | 0.93 | 0.73 | 0.70 | 1.02 | 1.02 | 0.75 | 0.47 |
| 103 | | | | | | 0.58 | 0.98 | 1.04 | 0.76 | 0.51 |
| 105 | 1.07 | 1.46 | 1.43 | 0.97 | 0.67 | | | | | |
| 116 | | | | | | 0.68 | 0.97 | 0.93 | 0.71 | 0.45 |
| 120 | 1.27 | 1.46 | 1.42 | 1.11 | 0.71 | | | | | |
| 135 | 1.09 | 1.54 | 1.35 | 1.22 | 0.86 | 0.60 | 0.98 | 1.04 | 0.76 | 0.51 |
| 150 | 1.08 | 1.59 | 1.77 | 1.40 | 0.98 | 0.67 | 1.09 | 0.96 | 0.73 | 0.48 |

are those expected for compound-nuclear reactions such as exemplified in Fig. 1. In general, the particles with energies not too far above the maxima in their respective spectra are most apt to arise from compound-nuclear events; the very high-energy particles are more suspect. Of even greater utility, though, is the requirement that the angular distribution in the c.m. system of particles emitted in compound-nuclear events be symmetric about a plane normal to the direction of the incident beam. Non-compound-nuclear events are nearly always expected to give particles preferentially emitted in the forward hemisphere; thus if the angular distributions exhibit any asymmetry, it is the particles emitted in the backward hemisphere that are likely to arise from compound-nuclear events.

Accordingly, the range of validity of the Bohr-independence hypothesis for nuclear reactions in the continuum was investigated in a differential fashion by measuring the energy and angular distributions of the protons and $\alpha$ particles emitted in the two reaction systems[21]:

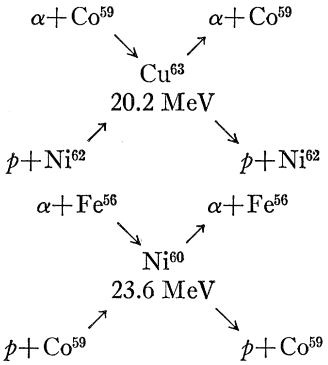


The experimental results, described below, indicate an apparent violation of the independence hypothesis. The implications for this apparent violaton arising from the mismatch of angular momentum and isotopic spin in corresponding entrance channels are examined in the discussion.

[21] These two reaction systems have also been investigated by C. Stephan and J. Huizenga (private communication).

## EXPERIMENTAL PROCEDURES

### General Procedures

The compound systems chosen for these experiments were $Cu^{63}$ at an excitation energy of 20.2 MeV and $Ni^{60}$ at an excitation energy of 23.6 MeV. Each was produced by corresponding proton and $\alpha$-particle irradiations. Proton beams were obtained from the Rutgers tandem Van de Graff and the Columbia University 37-in. cyclotron. The $\alpha$-particle beams were obtained from the Yale heavy-ion linear accelerator. Thus, the $Cu^{63}$ compound nucleus was formed with 14.3-MeV protons and 15.4-MeV $\alpha$ particles; the $Ni^{60}$ compound nucleus was formed with 14.3-MeV protons and 18.6-MeV $\alpha$ particles.

The targets required for these experiments ($Co^{59}$, $Fe^{56}$, and $Ni^{62}$) were self-supporting foils obtained from Oak Ridge National Laboratories, the uniformity and thickness of which were checked by measuring the energy loss of 5.48-MeV $\alpha$ particles that passed through them.[22,23] (The thinnest target used was 0.9 mg/cm$^2$.)

The experimental beam energy and the effective beam resolution for a given experiment were determined by observing the appropriate elastically scattered particles in an energy-calibrated solid-state detector. The average energy of the observed elastic peak was corrected for the average energy lost by the particle in the target after scattering.[22] This energy was then used to calculate the beam energy at the center of the target from the kinematics of scattering. The observed resolution of the elastically scattered beam was taken to be an estimate of the over-all energy resolution of the incident beam.

The energy spectra of protons and $\alpha$ particles emitted from the targets were measured at several angles from 30° to 160° with respect to the beam axis. A $\Delta E$-$E$ solid-state charged-particle detection telescope was

[22] National Association of Science, Report No. 39, Publication No. 1133, Washington, D. C., 1964 (unpublished); G. F. Williamson, J. P. Boujot, and J. Picard, Report No. CEA-R-3042, 1964 (unpublished).

[23] J. D'Auria, M. Fluss, L. Kowalski, and J. Miller, Phys. Rev. **168**, 1224 (1968).

TABLE IV. The c.m. cross sections are in units of mb/sr for intervals of 1-MeV channel energy. They are estimated to be accurate to ±10%.

| Energy interval $\theta_{lab}$ (deg) | Cross sections in 1-MeV intervals in mb/sr $Fe^{56}(\alpha, p)Co^{59}$ 6–7 | 7–8 | 8–9 | 9–10 | $Co^{59}(p, p')Co^{59}$ 6–7 | 7–8 | 8–9 | 9–10 |
|---|---|---|---|---|---|---|---|---|
| 45 | | | | | 6.84 | 4.84 | 3.05 | 3.15 |
| 52 | 3.74 | 2.32 | 1.40 | 0.96 | | | | |
| 60 | 3.56 | 2.24 | 1.39 | 0.82 | 4.88 | 3.66 | 3.28 | 2.49 |
| 75 | 3.34 | 2.04 | 1.27 | 0.64 | 4.24 | 3.20 | 2.35 | 1.80 |
| 90 | 3.37 | 2.03 | 1.22 | 0.62 | 4.39 | 3.08 | 2.18 | 1.63 |
| 100 | | | | | 4.34 | 3.00 | 2.18 | 1.51 |
| 105 | 3.23 | 2.02 | 1.16 | 0.60 | | | | |
| 110 | | | | | 4.31 | 3.00 | 2.12 | 1.53 |
| 120 | 3.35 | 2.11 | 1.19 | 0.61 | 4.42 | 3.04 | 2.07 | 1.50 |
| 135 | 3.52 | 2.16 | 1.25 | 0.63 | 4.37 | 2.93 | 1.97 | 1.33 |
| 145 | | | | | 4.38 | 3.00 | 1.96 | 1.27 |
| 150 | 3.56 | 2.24 | 1.36 | 0.717 | | | | |
| 160 | | | | | 4.46 | 3.09 | 1.93 | 1.26 |

TABLE V. The various optical-model parameters for the first three columns were obtained from Hodgson.[a] The last column of parameters comes from the work of Budzanowski *et al.*[b] The diffuseness for the potentials, Saxon-Woods (SW) and surface Gaussian (SG), are indicated in the parentheses.

| Parameter | Optical-model parameters Neutrons | Protons | $\alpha$ particles | $\alpha$ particles |
|---|---|---|---|---|
| Real potential $U$ (MeV) | $48-0.3E$ | $58-0.3E$ | 40 | 92.5 |
| Form of real potential $f(r)$ | SW(0.65) | SW(0.65) | SW(0.65) | SW(0.52) |
| Imaginary potential $W$ (MeV) | $3E^{1/2}$ | $3E^{1/2}$ | 12 | 15 |
| Form of imag. potential $g(r)$ | SG(0.98) | SG(0.98) | SW(0.65) | SW(0.52) |
| Radius $R$ (F) | $r_0A^{1/3}$ | $r_0A^{1/3}$ | $r_0A^{1/3}$ | $r_0A^{1/3}+1.11$ |
| Coulomb radius $R_C$ (F) | $r_0A^{1/3}$ | $r_0A^{1/3}$ | $r_0A^{1/3}$ | $\sim 5.22$ |
| Real spin orbit potential $U_s$ (MeV) | 19 | 19 | 0 | 0 |
| Imag. spin orbit potential $W_s$ (MeV) | 0 | 0 | 0 | 0 |
| $r_0$ $r_0$ (F) | 1.25 | 1.25 | 1.25 | 1.25 |

[a] P. E. Hodgson, in *Proceedings of the Conference on Direct Interactions and Nuclear Reaction Mechanisms*, edited by E. Clementel and C. Villi (Gordon and Breach, Science Publishers, Inc., New York, 1963), p. 103.
[b] A. Budzanowski *et al.*, (unpublished).

TABLE VI. Comparisons among experimental values for ratios of cross sections with those calculated including conservation angular momentum [calculated $(J)$] as well as those calculated including both conservation of angular momentum and of isotopic spin [calculated $(J, T)$].

| | $\frac{\sigma Co^{59}(\alpha, p)Ni^{2}(5\text{–}8\text{ MeV})}{\sigma Co^{59}(\alpha, \alpha')Co^{59}(7\text{–}12\text{ MeV})}$ | $\frac{\sigma Ni^{2}(p, p')Ni^{62}(5\text{–}8\text{ MeV})}{\sigma Ni^{62}(p, \alpha)Co^{59}(7\text{–}12\text{ MeV})}$ |
|---|---|---|
| | $Cu^{63}$ system | |
| Experimental | (1.25±0.06) | (3.4±0.3) |
| Calculated $(J)$ | 1.57 | 1.44 |
| Calculated $(J, T)$ | 1.35 | 2.66 |
| | $\frac{\sigma Fe^{56}(\alpha, p)Co^{59}(5\text{–}9\text{ MeV})}{\sigma Fe^{56}(\alpha, \alpha')Fe^{5}(7\text{–}12\text{ MeV})}$ | $\frac{\sigma Co^{59}(p, p')Co^{59}(5\text{–}9\text{ MeV})}{\sigma Co^{59}(p, \alpha)Fe^{56}(7\text{–}12\text{ MeV})}$ |
| | $Ni^{60}$ system | |
| Experimental | (1.9±0.1) | (4.2±0.4) |
| Calculated $(J)$ | 2.15 | 2.37 |
| Calculated $(J, T)$ | 1.79 | 3.86 |

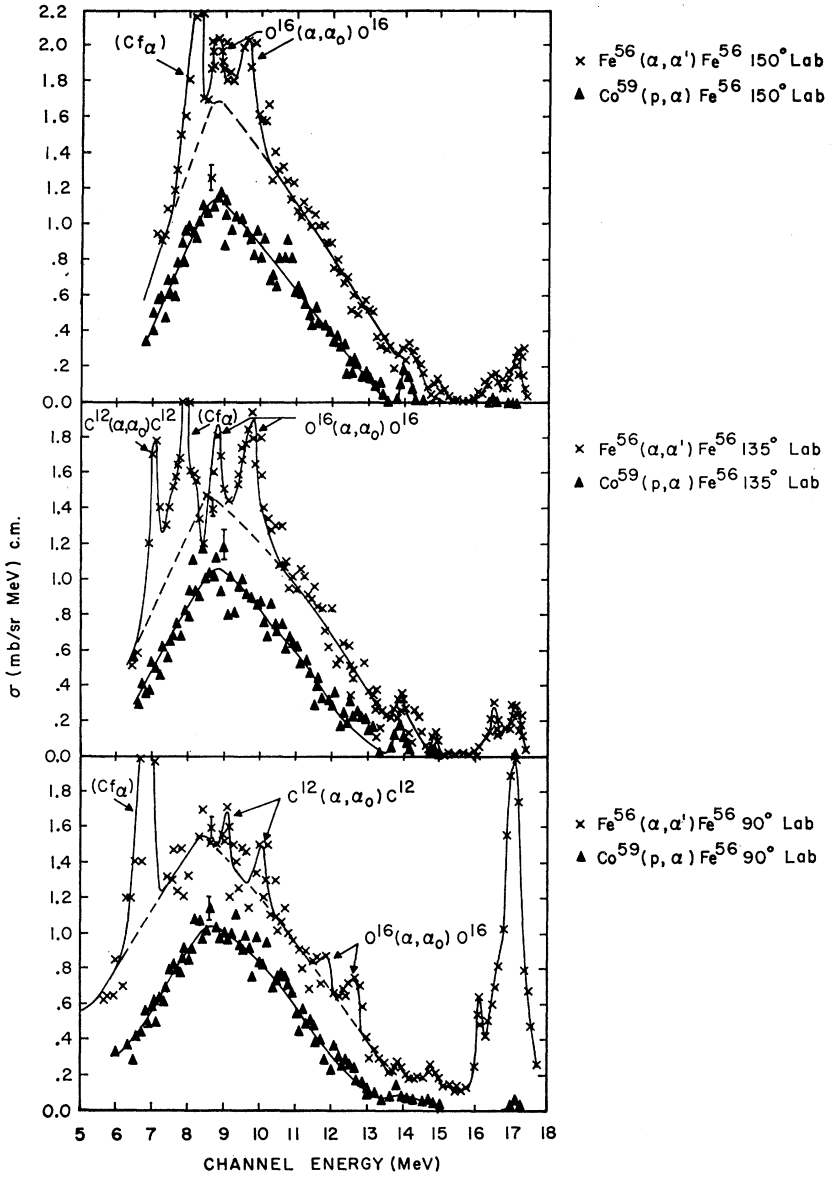


FIG. 3. Typical energy spectra for the reactions $Fe^{56}(\alpha, \alpha')Fe^{56}$ and $Co^{59}(p, \alpha)Fe^{56}$. See Fig. 1 for explanation of the dashed line.

used for particle identification in a manner that was previously described.[23] Previous measurements by other investigators were repeated so as to provide a check on the accuracy of the entire experimental setup.

The angular distributions for the $C^{12}(\alpha, p)N^{15}$ reaction at several energies were measured and were found to agree with previous work.[24] The measured $Co^{59}(p, \alpha)Fe^{56}$ energy spectra were found to be in agreement with those measured by Sherr and Brady.[25] The elastic and inelastic scattering to the first excited state in the $C^{12}(p, p')C^{12}$ reaction[26] provided an over-all check on the accuracy of the measurements of the charged-particle energy spectra in the proton-induced reactions.

### Conversion to the Center of Mass

The transformation of the experimental results to the barycentric system was accomplished through the use of slightly modified versions of the codes NEWDAC[27] and KINEMATICS.[28] Correction for the energy loss of the emitted particles in the target is included in NEWDAC. The results are reported as $d^2\sigma/d\Omega dE_{\text{chan}}$ versus $E_{\text{chan}}$ at a laboratory angle $\theta$ which is usually within a few degrees of the corresponding barycentric angle.

[24] J. R. Priest, D. J. Tendam, and E. Bleuler, Phys. Rev. **119**, 1301 (1960).
[25] R. Sherr and F. P. Brady, Phys. Rev. **124**, 928 (1961).
[26] G. Temmer (private communication).
[27] J. B. Ball, Oak Ridge National Laboratory Report No. ORNL-3405-UC34, 1963 (unpublished).
[28] J. B. Ball, Oak Ridge National Laboratory Report No. ORNL-3251-UC34, 1962 (unpublished).

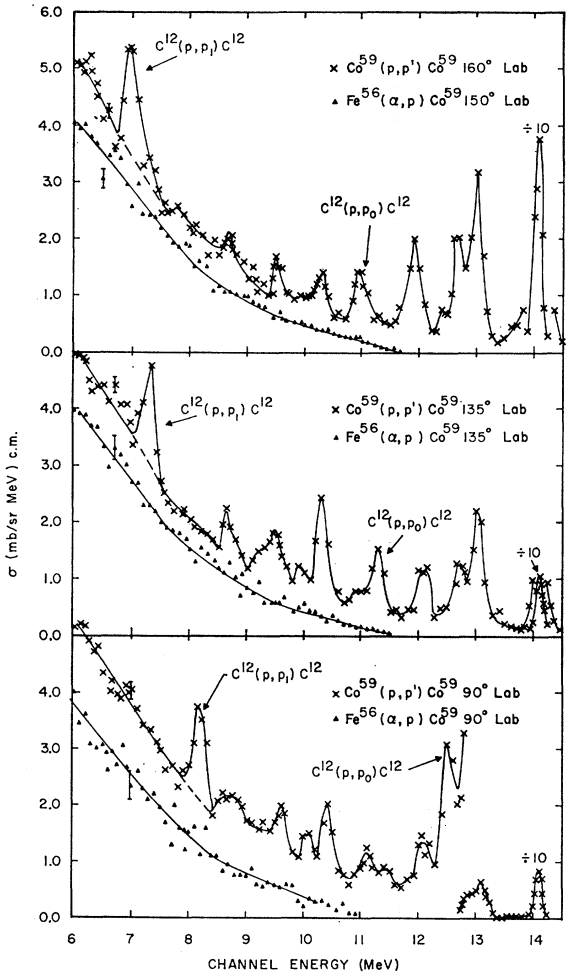


FIG. 4. Typical energy spectra for the reactions $Fe^{56}(\alpha, p)Co^{59}$ and $Co^{59}(p, p')Co^{59}$. See Fig. 1 for explanation of the dashed line.

## EXPERIMENTAL RESULTS

The measured energy spectra of the protons and $\alpha$ particles emitted at various angles in the regions of overlapping levels are given for 1-MeV intervals in Tables I–IV. In Figs. 1–4 are shown some of the typical energy spectra which were obtained in these experiments.

### Corrections for Spurious Events

Particles resulting from reactions with $C^{12}$ and $O^{16}$ contamination adsorbed on the targets were identified by their distinct kinematics. In a number of spectra, double peaks which corresponded to reactions of the contaminants could be resolved. These double peaks are understood when it is realized that the contaminants were concentrated on both surfaces of the targets. The contamination peaks were subtracted graphically from the energy spectra in which they appeared. This graphical subtraction is indicated by the dashed lines in Figs. 1–4. It is estimated that the removal of the contamination peaks introduces an error of no more than 5%.

A limitation on the accuracy of the data arose from low-energy "tails" caused by the intense elastic scattering peaks at forward angles. These tails are attributed to small-angle scattering of the elastically scattered particles in the detector slits. Their contribution to the continuum part of the $(\alpha, \alpha')$ and $(p, p')$ spectra could not be unambiguously removed. Thus, the energy spectra forward of 60° were not considered in the final analysis of the $(\alpha, \alpha')$ and $(p, p')$ spectra.

The background counting rate was measured by collecting the resulting background spectra when no target was in position. This spectrum was then subtracted from the energy spectra collected with the target. The background counting rate was usually less than 2% of the counting rate with target.

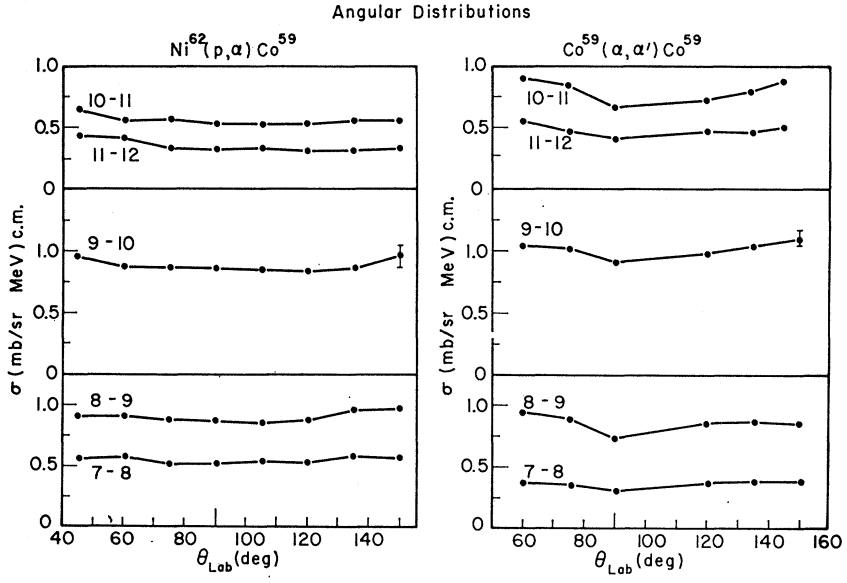


FIG. 5. Angular distributions in indicated intervals of channel energies for the reactions $Co^{59}(\alpha, \alpha')Co^{59}$ and $Ni^{62}(p, \alpha)Co^{59}$.

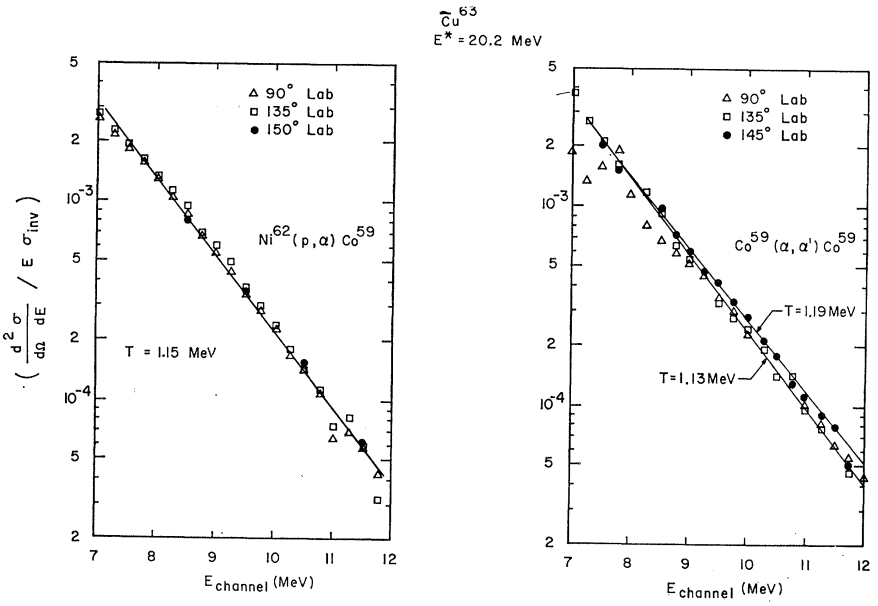


FIG. 6. Nuclear temperature plots for the reactions $Co^{59}(\alpha, \alpha')Co^{59}$ and $Ni^{62}(p, \alpha)Co^{59}$.

### Systematic and Random Errors

The following discussion of the various systematic and random errors gives the limits on the accuracy of the differential cross sections that are reported.

The statistical variations for each $\frac{1}{4}$-MeV interval caused by the finite number of events recorded were usually less than $\pm 8\%$ at the maximum of the continuum spectra. Many spectra had statistical variations considerably smaller than this. The chance-coincidence counting rates were usually negligible. Dead time in the multichannel analyzers were less than 2%.

The uncertainty in the solid angle subtended by the counter telescope as determined by the use of an $Am^{241}$ point source of known activity is estimated to be less than $\pm 3\%$. An additional error of $\pm 2\%$ in the solid angle is introduced by the finite size of the beam spot. The variations in the target thicknesses were less than $\pm 3\%$ as measured by the energy loss for transmitted $\alpha$ particles from $Am^{241}$. The projectile beams collected in the Faraday cup were assumed to be fully ionized and the total beam current measured with a current integrator. The current integrator was calibrated to within $\pm 1\%$ and the current drift during long periods of data collection was of the order of $\pm 4\%$ of the total current. The scattering of the beam out of the acceptance angle of the Faraday cup by the target foil was negligible.

The absolute energy calibration of the telescope and the associated electronics was accurate to $\pm 1\%$. The beam energy was monitored at frequent intervals during the experimental runs. The uncertainty in the measurement of the beam energy was $\pm 3\%$. Changes in the beam energy usually did not exceed this 3% uncertainty.

The reproducibility of the data indicates that an error of about $\pm 5\%$ is reasonable for the reported ratios of cross sections $\sigma(x, p)/\sigma(x, \alpha)$ when $x$ is an $\alpha$ particle and $\pm 10\%$ when $x$ is a proton. The difference in these reproducibilities is consistent with the fact that the $\alpha$-particle induced spectra were collected simultaneously while the proton induced spectra were collected during separate bombardment periods using different scattering chambers.

### Comparison of Corresponding Spectra

A diagnostic tool that allows one to relate the shapes of corresponding energy spectra is needed in the analysis of the data. [For example, one might desire to compare the shape of the $Co^{59}(\alpha, \alpha')Co^{59}$ energy spectra to the $Ni^{62}(p, \alpha)Co^{59}$ energy spectra.] The *apparent* nuclear temperature that characterizes each spectrum was used for this purpose. This quantity was determined for each spectrum in the usual manner[2] from a plot of $\log[(d^2\sigma/d\Omega dE_{\text{chan}})(1/\sigma_i E_{\text{chan}})]$ versus $E_{\text{chan}}$.

The inverse cross sections $\sigma_i$ required for this treatment were obtained from ABACUS II[29] with the parameters given in Table V. Although the values of the nuclear temperatures obtained in this way are sensitive

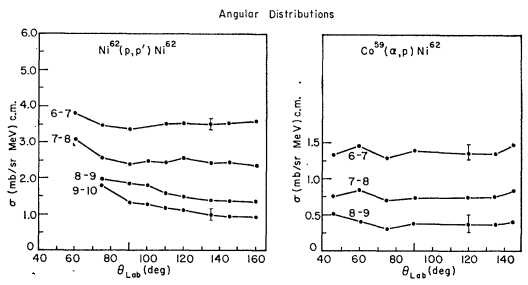


FIG. 7. Angular distributions in indicated intervals of channel energies for the reactions $Co^{59}(\alpha, p)Ni^{62}$ and $Ni^{62}(p, p')Ni^{62}$.

[29] E. H. Auerbach, Brookhaven National Laboratory Report No. BNL-6562 (1964).

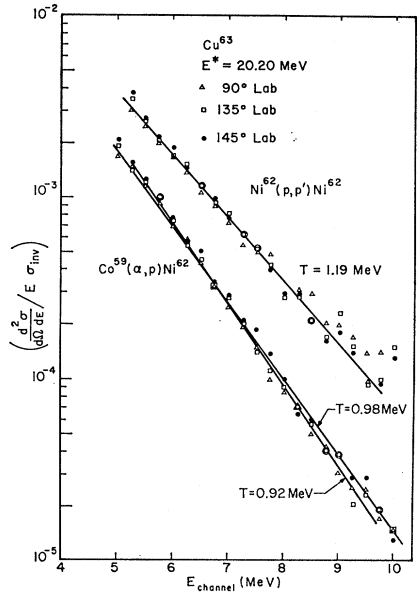


FIG. 8. Nuclear temperature plots for the reactions $Co^{59}(\alpha, p)Ni^{62}$ and $Ni^{62}(p, p')Co^{59}$.

to the set of inverse cross sections which are used, the comparison of corresponding spectra is not sensitive to these cross sections, since corresponding spectra result in the same residual nucleus.

*$Cu^{63}$ system.* The energy spectra at several angles from the reactions $Co^{59}(\alpha, \alpha')Co^{59}$ and $Ni^{62}(p, \alpha)Co^{59}$ are compared in Fig. 1 and Table I. The total cross section for the emission of $\alpha$ particles in the energy interval 7–12 MeV is obtained by integrating the $\alpha$-particle energy spectra over angle from 90°–180° and over energy from 7 to 12 MeV and multiplying by 2. It is calculated from the data in this waythat the cross section for the $Co^{59}(\alpha, \alpha')Co^{59}$ reaction from 7 to 12 MeV is 43±4 mb and that for the $Ni^{62}(p, \alpha)Co^{59}$ reaction over the same interval of energy is 39±4 mb. A comparison of the angular distributions of these energy spectra is made in Fig. 5. Generally, these angular distributions are quite similar. However, detailed inspection reveals that the $Co^{59}(\alpha, \alpha')Co^{59}$ angular distributions are more anisotropic than the corresponding $Ni^{62}(p, \alpha)Co^{59}$ angular distributions.

A plot of $\log[(d^2\sigma/d\Omega dE_{\text{chan}})(1/\sigma_i E_{\text{chan}})]$ versus channel energy for the $Co^{59}(\alpha, \alpha')Co^{59}$ and $Ni^{62}(p, \alpha)Co^{59}$ energy spectra at several backward angles yields the reasonably straight lines shown in Fig. 6. The apparent nuclear temperatures for the $Co^{59}(\alpha, \alpha')Co^{59}$ energy spectra and the $Ni^{62}(p, \alpha)Co^{59}$ energy spectra are both about 1.15 MeV. A slight increase in the apparent nuclear temperature is observed for the $Co^{59}(\alpha, \alpha')Co^{59}$ spectra as one goes toward larger angles in the backward direction. The range of this change in the apparent nuclear temperature is from 1.13 to 1.19 MeV which is, however, within the experimental error for this quantity.

In Fig. 2 and Table II, the $Ni^{62}(p, p')Ni^{62}$ and the $Co^{59}(\alpha, p)Ni^{62}$ energy spectra are compared. Integrating these two sets of corresponding spectra over angle and from 5 to 8 MeV in the same way as described above, one obtains cross sections of 134±13 mb for the $Ni^{62}(p, p')Ni^{62}$ energy spectra and 54±5 mb for the $Co^{59}(\alpha, p)Ni^{62}$ energy spectra. It is clear from the data that the $(p, p')$ spectra indicate larger cross sections than do the corresponding $(\alpha, p)$ spectra.

The angular distributions for the $Ni^{62}(p, p')Ni^{62}$ and $Co^{59}(\alpha, p)Ni^{62}$ reactions (Fig. 7) are both reasonably isotropic except for some forward peaking in the $(p, p')$ data. This forward peaking is partly ascribed

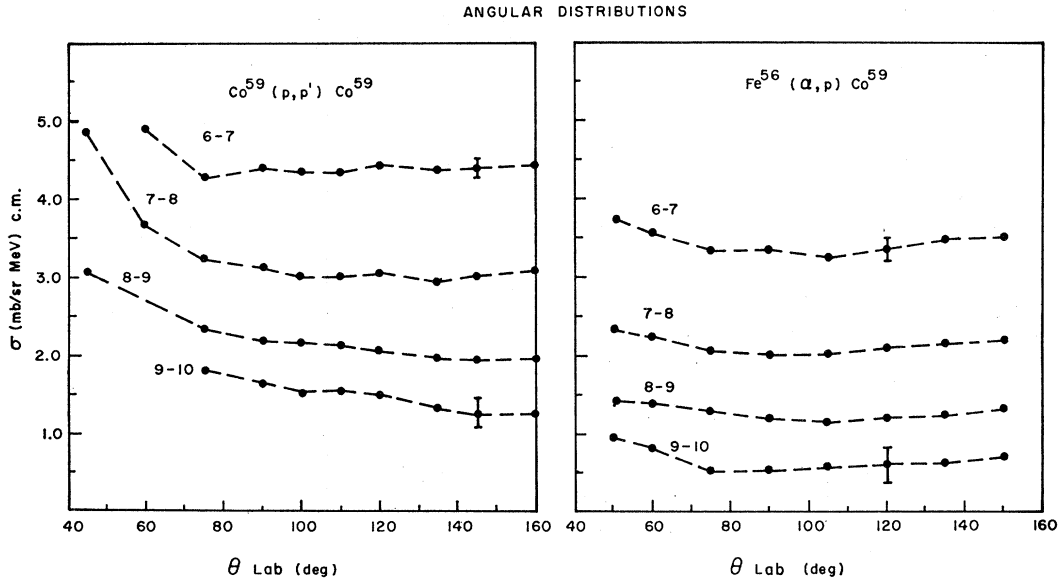


FIG. 9. Angular distributions in indicated intervals of channel energies for the reactions $Fe^{56}(\alpha, \alpha')Fe^{56}$ and $Co^{59}(p, \alpha)Fe^{56}$.

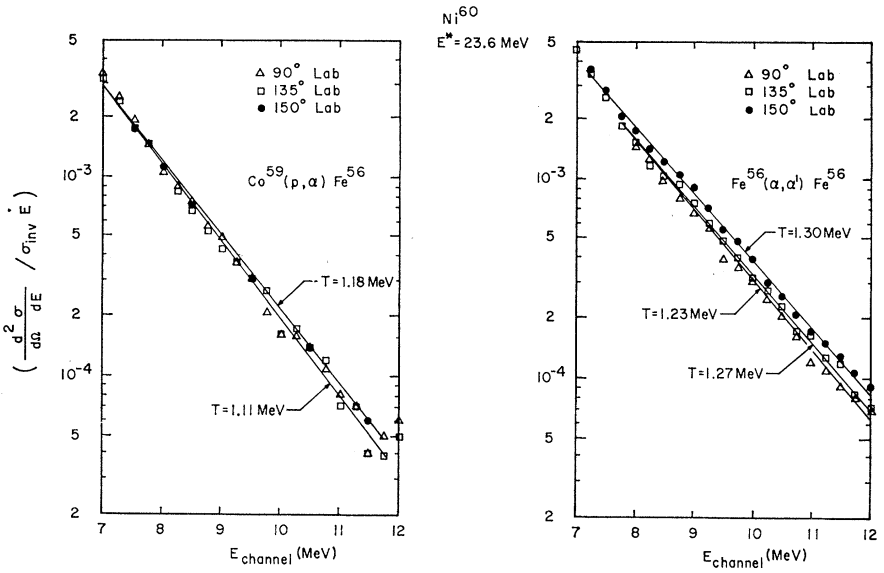


FIG. 10. Nuclear temperature plots for reactions $Fe^{56}(\alpha, \alpha')Fe^{56}$ and $Co^{59}(p, \alpha)Fe^{56}$.

to the tail effect from the elastic peak that was mentioned previously. For the most part, one can say that the $(p, p')$ and $(\alpha, p)$ reactions show isotropic angular distributions over the bulk of the continuum spectra.

Plots of $\log[(d^2\sigma/d\Omega dE_{\text{chan}})(1/\sigma_i E)]$ versus channel energy for the two sets of energy spectra result in fairly good straight lines (Fig. 8). The apparent nuclear temperature for the $Ni^{62}(p, p')N^{62}$ spectra and the $Co^{59}(\alpha, p)N^{62}$ spectra are 1.19 MeV and 0.92–0.98 MeV, respectively.

*$Ni^{60}$ system.* The energy spectra from the two corresponding reactions, $Fe^{56}(\alpha, \alpha')Fe^{56}$ and $Co^{59}(p, \alpha)Fe^{56}$, are compared in Fig. 3 and Table III. Integrating these energy spectra over angle in the energy interval of 7–12 MeV, one obtains the cross sections of 75±8 mb for the $Fe^{56}(\alpha, \alpha')Fe^{56}$ reaction and 45±5 mb for the $Co^{59}(p, \alpha)Fe^{56}$ reaction. Thus, the $Fe^{56}(\alpha, \alpha')Fe^{56}$ energy spectra show that this reaction has a larger cross section than the corresponding $Co^{59}(p, \alpha)Fe^{56}$ reaction.

It can be seen from Fig. 9 that these two corresponding reactions do not exhibit identical angular distributions, the $Fe^{56}(\alpha, \alpha')Fe^{56}$ angular distributions being more anisotropic than the $Co^{59}(p, \alpha)Fe^{56}$ angular distributions.

Again, plots of $\log[(d^2\sigma/d\Omega dE_{\text{chan}})(1/\sigma_i E)]$ versus channel energy for these spectra lead to the straight lines shown in Fig. 10. For the $Fe^{56}(\alpha, \alpha')Fe^{56}$ energy spectra the apparent nuclear temperature ranges from 1.23 to 1.30 MeV, while for the $Co^{59}(p, \alpha)Fe^{56}$ energy spectra the nuclear temperature ranges from 1.11 to 1.18 MeV.

The corresponding proton energy spectra for the $Ni^{60}$ system, the $Co^{59}(p, p')Co^{59}$ energy spectra, and the $Fe^{56}(\alpha, p)Co^{59}$ energy spectra, are compared in Fig. 4 and Table IV. Integrating these energy spectra over angle and from 5 to 9 MeV one obtains cross sections of 188±19 mb for the $Co^{59}(p, p')Co^{59}$ reaction and 139±14 mb for the corresponding $Fe^{56}(\alpha, p)Co^{59}$ reaction. The $Co^{59}(p, p')Co^{59}$ spectra clearly show larger cross section than do the corresponding $Fe^{56}(\alpha, p)Co^{59}$ energy spectra.

Comparison of the angular distributions in the backward direction (Fig. 11) shows the proton energy spectra for both reactions are reasonably isotropic. Figure 12 shows the nuclear temperature plots. An apparent nuclear temperature of 1.3 MeV is found for the $Co^{59}(p, p')Co^{59}$ spectra, which is compared to and apparent nuclear temperature of 1.17 MeV found for the corresponding $Fe^{56}(\alpha, p)Co^{59}$ energy spectra.

The same set of corresponding reactions leading to the $Ni^{60}$ compound system at a higher excitation energy has recently been studied by Benveniste *et al.*[30] The results are in agreement with those presented here for those parts of the spectra which exclude two-particle emission.

## DISCUSSION

Individually, each of the charged-particle energy spectra corresponding to residual nuclei with excitation energies in the region of overlapping levels have a shape consistent with that expected for a compound nucleus reaction. That this is so may be seen from the straight line portions of the plots shown in Figs. 6, 8, 10, and 12. Further, except for the experimental problem with the spectra in the forward direction arising from elastic scattering, the angular distributions of the emitted charged particles are symmetric about $\frac{1}{2}\pi$ in the c.m. system. Thus, the spectra measured at angles greater than $\frac{1}{2}\pi$ were taken as the clearest example of those arising from compound-nuclear reactions.

Assuming that the excitation energy of the system is

[30] J. Benveniste, G. Merkel, and A. Mitchell, Phys. Rev. **174**, 1357 (1968).

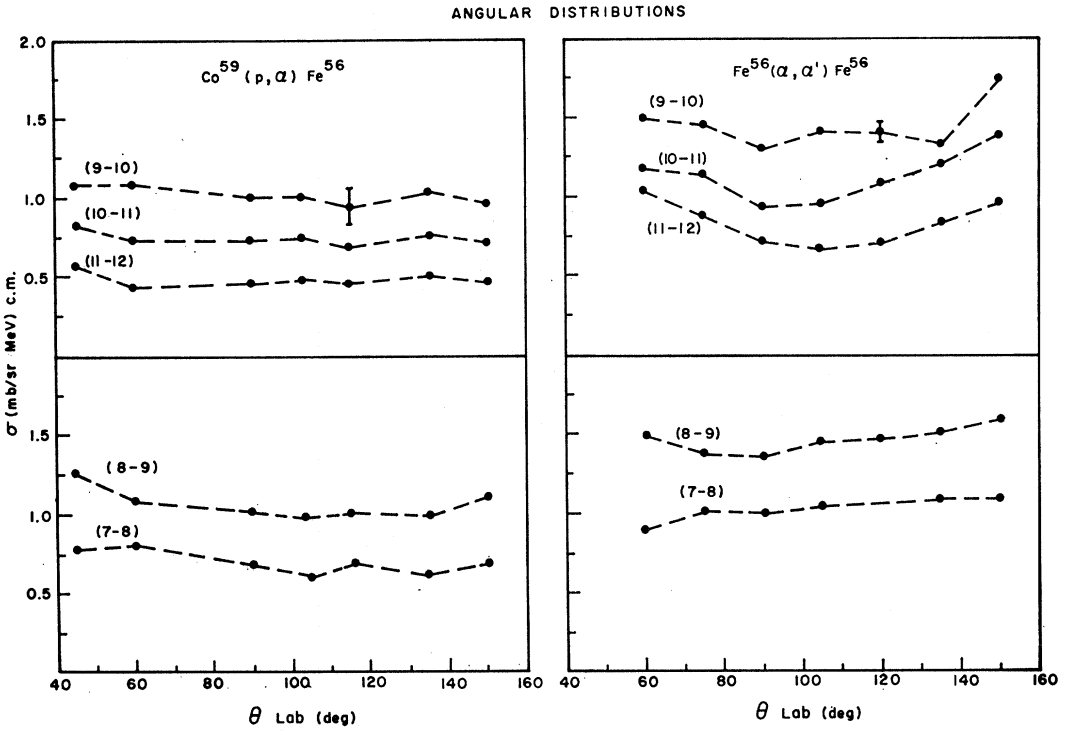


FIG. 11. Angular distributions in indicated intervals of channel energies for the reactions $Fe^{56}(\alpha, p)Co^{59}$ and $Co^{59}(p, p')Co^{59}$.

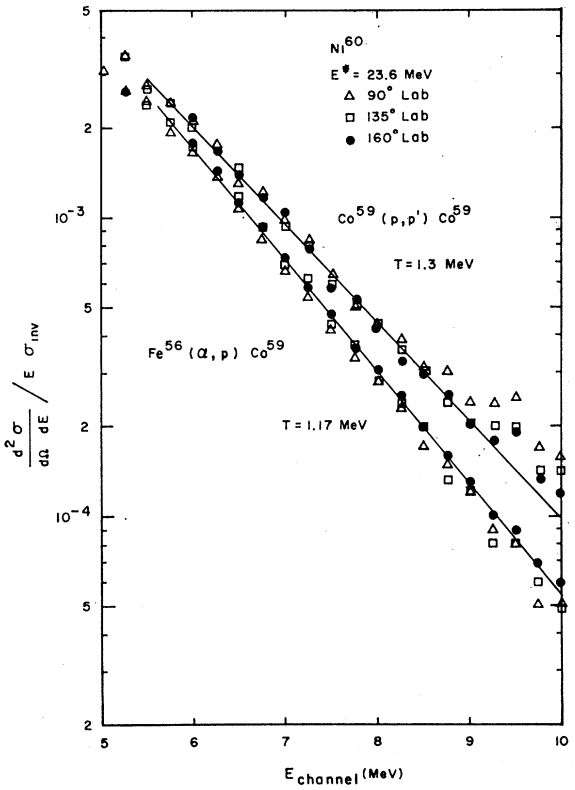


FIG. 12. Nuclear temperature plots for the reactions $Fe^{56}(\alpha, p)Co^{59}$ and $Co^{59}(p, p')Co^{59}$.

the only significant constant of the motion, the condition of independence of decay from the mode of formation demands that the ratio of cross sections, $\sigma(\alpha, p)/\sigma(\alpha, \alpha')$ and $\sigma(p, p')/\sigma(p, \alpha)$, be equal. For the $Cu^{63}$ system

$$\frac{\sigma(Co^{59}(\alpha, p)Ni^{62})\ (5\text{–}8\ \text{MeV})}{\sigma(Co^{59}(\alpha, \alpha)Co^{59})\ (7\text{–}12\ \text{MeV})} = 1.25$$

and

$$\frac{\sigma(Ni^{62}(p, p')Ni^{62})\ (5\text{–}8\ \text{MeV})}{\sigma(Ni^{62}(p, \alpha)Co^{59})\ (7\text{–}12\ \text{MeV})} = 3.40,$$

and for the $Ni^{60}$ system

$$\frac{\sigma(Fe^{56}(\alpha_j, p)Co^{59})\ (5\text{–}9\ \text{MeV})}{\sigma(Fe^{56}(\alpha, \alpha')Fe^{56})\ (7\text{–}12\ \text{MeV})} = 1.85$$

and

$$\frac{\sigma(Co^{59}(p, p')Co^{59})\ (5\text{–}9\ \text{MeV})}{\sigma(Co^{59}(p, \alpha)Fe^{56})\ (7\text{–}12\ \text{MeV})} = 4.20.$$

Thus both the $Cu^{63}$ system and the $Ni^{60}$ system exhibit an apparent violation of the independence hypothesis: In both systems the ratio of cross sections $\sigma(p, p')/\sigma(p, \alpha)$ is greater than the corresponding ratio of cross sections, $\sigma(\alpha, p)/\sigma(\alpha, \alpha')$. Further, the apparent nuclear temperatures that characterize the shapes of corresponding spectra are not always identical. These divergences immediately raise the question of whether the energy of the system is the only significant constant

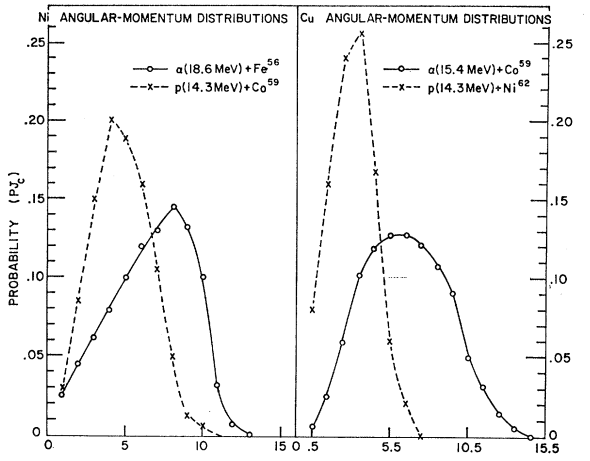


FIG. 13. Angular momentum distributions for the $Ni^{60}$ and the $Cu^{63}$ compound nuclei, formed by incident protons and $\alpha$ particles, as calculated with ABACUS II. Angular momentum is in units of $\hbar$.

of the motion; and, if it is not, whether the other constants of the motion are identical for the corresponding entrance channels of the two systems. The constants of the motion that will first be considered are energy and angular momentum; the possibility and consequences of isotopic spin conservation will be considered later.

The kinetic energies of the protons and $\alpha$ particles in the two corresponding entrance channels were specifically chosen so that the excitation energies (relative energy plus binding energy) would be the same. The energy resolution was of the order of 0.2–0.5 MeV; therefore, differences in corresponding energy spectra due to Ericson fluctuations were not considered. Further, experimental runs were carried out in which the energies of the incoming projectiles were varied by 0.5 MeV. Variations in the reported ratio of cross sections were insensitive to this change in energy.

With corresponding incident energies, however, the distributions of angular momenta of the compound nuclei that are formed are not the same. Moreover, if the isotopic spin of the target in the incident $\alpha$-particle channel is taken as $T$, then the isotopic spin of that entrance channel has only one value which is also $T$. For the corresponding proton entrance channel (the target isotopic spin being $T+\frac{1}{2}$), two values of isotopic spin are possible: either $T$ or $T+1$. Thus, neither angular momenta nor isotopic spin distributions are the same in the corresponding entrance channels. The purpose, then, of the following two sections is to investigate whether the apparent violations of the independence hypothesis that have been observed can arise from these differences in the constants of motion in the corresponding bombarding system.

### Angular Momentum Conservation

The general formalism for the inclusion of angular momentum conservation within the framework of the statistical model for nuclear reactions is well known.[31] The particular formulation that is used in this study to investigate the effects of angular momentum conservation has been embodied in a computer program called EVAMCO which is similar to the work of Dudley *et al.*[31] At this juncture, the general way in which angular momentum conservation may be included within the context of the statistical model will be briefly described.

We begin by writing the cross section for going from the set of entrance channels characterized by particle $a$ to the set of exit channels characterized by particle $b$ as[32]

$$\sigma(a, b) = \sum_J \sigma(J, U/a) W(b/J, U), \quad (1)$$

where $\sigma(J, U/a)$ is the cross section to form the compound nucleus with excitation energy $U$ and of spin $J$ from particle $a$, and $W(b/J, U)$ is the probability that a compound nucleus characterized by spin $J$ and energy $U$ will decay via particle $b$. There is, of course, a similar expression for going from a corresponding set of entrance channels characterized by particle $a'$ to the same set of exit channels $b$.

$$\sigma(a', b) = \sum_J \sigma(J, U/a') W(b/J, U). \quad (1')$$

The independence hypothesis is manifest in this expression in that the quantity $W(b/J, U)$ depends on the entrance channel *only* through the conserved quantities $J$ and $U$; the sum, however, will not, in general, exhibit independence unless $W(b/J, U)$ is independent of $J$. Indeed, it is just this dependence of $W(b/J, U)$ on $J$ that is the cause of the angular-momentum-conserving effects. It is clear, then, that the objective of any angular-momentum-conserving calculation is to determine the terms $\sigma(J, U/a)$ and $W(b/J, U)$.

It should be pointed out that the conventional test of the independence hypothesis will be valid if two corresponding sets of entrance channels characterized by particles $a$ and $a'$, give compound nuclei with the same distribution of angular momenta:

$$\frac{\sigma(J, U/a)}{\sigma(U/a)} = \frac{\sigma(J, U/a')}{\sigma(U/a')}, \quad (2)$$

---

[31] T. Ericson, Advan. Phys. **9**, 425 (1960); D. C. Williams and T. D. Thomas, Nucl. Phys. **92**, 1 (1967); N. D. Dudey and T. T. Sugihara, Phys. Rev. **139**, B896 (1965); D. G. Sarantites and B. D. Pate, Nucl. Phys. **93**, 545 (1967); **93**, 567 (1967); A. C. Douglas and N. MacDonald, *ibid.* **13**, 382 (1959).

[32] The polarization of the compound nucleus must also be conserved; that is, the $J_z$ component of the angular momentum. Equation (1) does not include $J_z$. This is because Eq. (1) is valid for the set of exit channels $b$ when these exit channels are defined by $4\pi$ geometry. For example, $b$ *may not* represent protons between 5 and 8 MeV at $\theta=150°$; but, it *may* represent protons between 5 and 8 MeV integrated over the polar and azimuthal angles. Since the objective is to compare the continuum cross section integrated over angles in order to validate the independence hypothesis, expressions such as Eq. (1) are of the least complicated form which are required for this purpose.

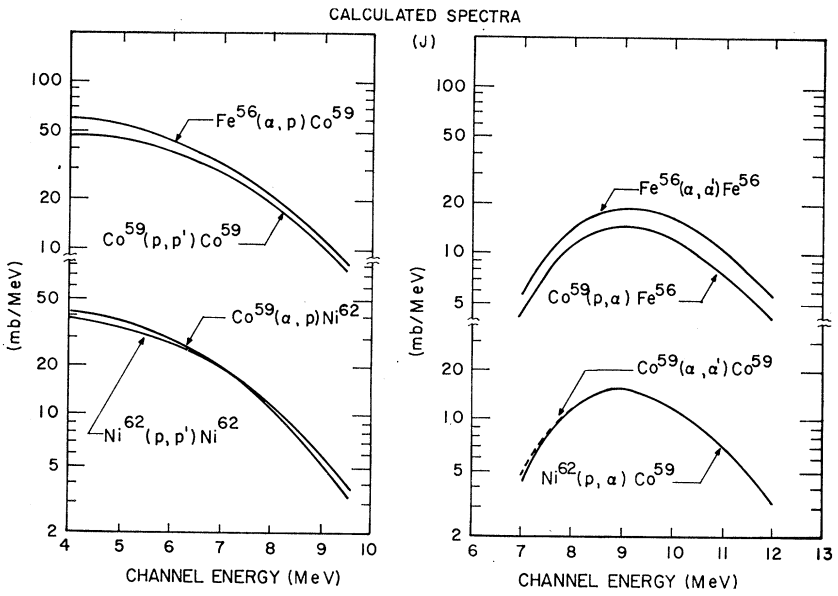


FIG. 14. Calculated proton and $\alpha$-particle energy spectra with angular momentum conserved.

for all values of $J$, where

$$\sigma(U/a)=\sum_J \sigma(J, U/a), \tag{2'}$$

$$\sigma(U/a')=\sum_J \sigma(J, U/a'). \tag{2''}$$

The ratio of cross sections for two competing sets of exit channels distinguished by particles $b$ and $c$, may be written

$$\frac{\sigma(a, b)}{\sigma(a, c)}=\frac{\sum_J \sigma(J, U/a)W(b/J, U)}{\sum_J \sigma(J, U/a)W(c/J, U)}. \tag{3}$$

Substituting (2) into (3), one obtains

$$\frac{\sigma(a, b)}{\sigma(a, c)}=\frac{\sum_J \sigma(J, U/a')[\sigma(U/a)/\sigma(U/a')]W(b/J, U)}{\sum_J \sigma(J, U/a')[\sigma(U/a)/\sigma(U/a')]W(c/J, U)} \tag{4}$$

$$\sigma(a, b)/\sigma(a, c)=\sigma(a', b)/\sigma(a', c). \tag{4'}$$

Equation (4') represents the usual experimental test for independence; however, this result is obtained only if Eq. (2) is valid.

The two sets of corresponding entrance channels in this work do *not* conform to Eq. (2) (see Fig. 13), nor was there any *a priori* reason to believe that the effect of the $J$ dependence of the $W$ terms, as reflected in the ratio of cross sections, was small; thus it was necessary to calculate the quantities $\sigma(J, U/a)$ and $W(b/J, U)$ for the channels of interest.

The cross sections $\sigma(J, U/a)$ are determined from the spins of the projectile and target nuclei and the transmission coefficients $T_l$ for reaction with entrance channel partial waves of angular momentum $l$. These transmission coefficients were calculated with the ABACUS II[29] program using the optical-model parameters given in Table V.

The quantities $W(b/J, U)$ depend both on the $T_l$ that characterize the various competing exit channels and on the level densities of the compound and residual nuclei. The exit-channel transmission coefficients were also computed with the ABACUS II program. The level density of a nucleus with spin $J$ and excitation energy $U$ was taken to be

$$\Omega(U, J)=\frac{(2J+1)(U-\delta)^{-1.25}}{\pi^{1/2}(2IT\hbar^2)^{3/2}} \times \exp\left(2a^{1/2}(U-\delta)^{1/2}\frac{-J(J+1)\hbar^2}{2IT}\right). \tag{5}$$

The quantity $a$ is the usual level-density parameter[2] which was taken here to be 1/11 times the mass number of the nucleus; $\delta$ is a term that attempts to correct for the pairing-energy effect on level density[33]; $I$ is the effective moment of inertia; and $T$, the temperature of the nucleus, is given by the expression

$$U=aT^2-T.$$

Thus, there are three parameters $a$, $\delta$, and $I$ that enter into the calculation of $\Omega(U, J)$.

The important point to be made is that for a wide range of values for these parameters the differences in shape between calculated corresponding spectra are in qualitative agreement with the observed differences in shapes between corresponding spectra for both the $Cu^{63}$ and $Ni^{60}$ compound systems.

Figure 14 illustrates calculated energy spectra for the compound systems $Cu^{63}$ and $Ni^{60}$, while Fig. 15 shows typical experimental spectra at backward angles. For both the calculated and experimental results, the $(p, p')$ spectrum is harder than that for the corresponding $(\alpha, p)$, while the $(\alpha, \alpha')$ spectrum is harder than that

[33] I. Dostrovsky, Z. Fraenkel, and G. Friedlander, Phys. Rev. 116, 683 (1960).

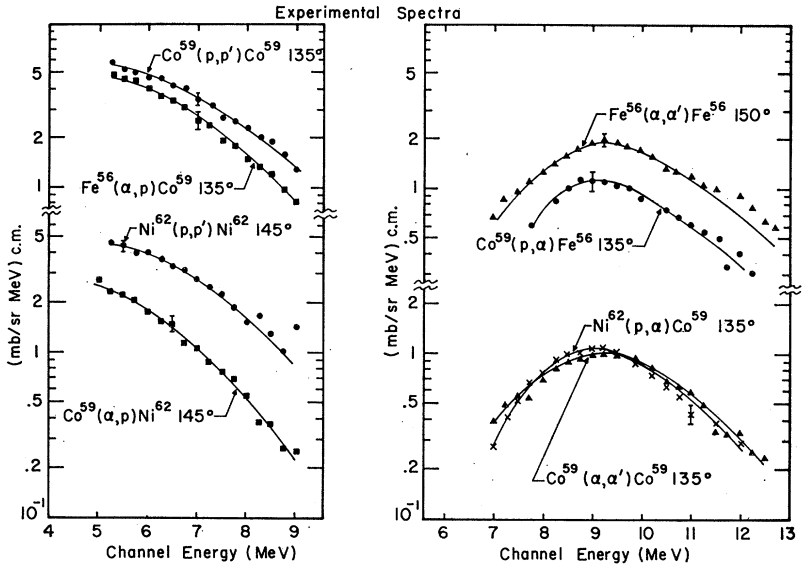


FIG. 15. Typical experimental proton and α-particle energy spectra.

for the corresponding $(p, \alpha)$. Thus, if the observed differences in shapes of corresponding spectra were the only divergence from the independence hypothesis, it could be reinstated by correcting for the effects due to the difference in the angular momentum spectra in corresponding entrance channels. The relative magnitudes, though, of the measured cross sections obviate this possibility.

As usual, the ratios of probabilities for the emission of various particles from an excited compound-nucleus are particularly sensitive to the effects of the odd and even character of the neutron and proton number on the level densities of the resulting residual nuclei. This effect may be approximated by assigning a pairing energy $\delta$ to each nucleus that defines a "characteristic level" above which the excitation energies that appear in level-density formulas are measured.[33] For example, if $\delta$ for $Ni^{62}$ is changes from 0 to 2.81 MeV, while that for $Cu^{62}$ is kept (as usual for odd-odd nuclei) at zero, the ratio of calculated probabilities for proton and neutron emission from a $Cu^{63}$ compound nucleus at an excitation energy of 20.2 MeV goes from $\sim 2$ to $\sim 0.2$. The effect of $\delta$ is fairly insensitive to the spin of the compound nucleus and thus will be much the same for corresponding entrance channels.

On the other hand, the effective moment of inertia $I$ which appears explicitly in the expression for the spin-dependent level density [Eq. (5)] can also have a large effect on the relative probabilities of emitting various particles which is particularly significant for the higher-spin compound nuclei. Thus, the effect will be much less in the proton reaction system than in the $\alpha$ reaction system because of the difference in the spin distribution of the compound nuclei that are formed in the two sets of entrance channels. For example, diminishing the effective moment of inertia of the residual $Co^{59}$ nucleus from that for a rigid body to a value that is 30% of that for a rigid body increases the calculated cross section for the $Co^{59}(\alpha, \alpha')Co^{59}$ reaction by about a factor of 4 while leaving the corresponding cross section for the $Ni^{62}(p, \alpha)Co^{59}$ reaction essentially unchanged. In general, calculations of the behavior of $Cu^{63}$ nuclei formed via the two systems considered here indicate that a lowering of the effective moment of inertia will enhance cross sections for $(\alpha, \alpha')$ reactions, diminish those for $(\alpha, p)$ reactions, and have little effect on the $(p, \alpha)$ and $(p, p')$ reactions. At first glance, it might appear that this is just the effect that is required because diminishing the moment of inertia will then cause the ratio $\sigma(\alpha, p)/\sigma(\alpha, \alpha')$ to be less than the corresponding ratio $\sigma(p, p')/\sigma(p, \alpha)$, which is indeed the direction of the observed divergence. However, it would also mean that the cross section for the $Co^{59}(\alpha, \alpha')Co^{59}$ reaction would be several times larger than that for the $Ni^{62}$ $(p, \alpha)Co^{59}$ reaction unless the total reaction cross section of 14.3-MeV protons with $Ni^{62}$ is several times larger than that for 15.4-MeV $\alpha$ particles with $Co^{59}$. Neither of these implications is true. From Fig. 1 it may be seen that the cross sections sections for the two corresponding reactions for emitted $\alpha$ particles between 7 and 12 MeV differ by only about 10%. The total reaction cross section for 15.4-MeV $\alpha$ particles with $Co^{59}$ is about 920 mb,[23] while that for 14.5-MeV protons is about 1070 mb[34]; again, a difference of less than 20%.

To sum up the effects of pairing energy and angular momentum:

(i) The requirement of angular momentum conservation leads to results that are in qualitative agreement with the differences in the shapes of the spectra of particles emitted in corresponding reactions.

[34] J. F. Dicello, G. J. Igo, and M. L. Roush, Phys. Rev. **157**, 1001 (1967).

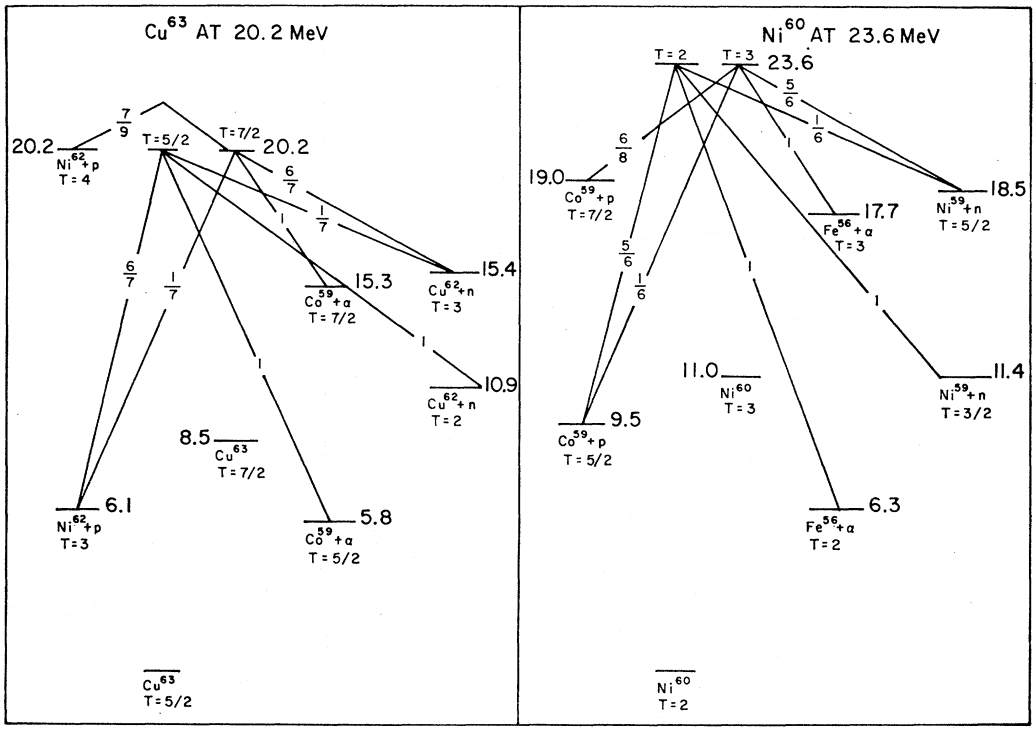


FIG. 16. Ground-state level scheme of $T_>$ and $T_<$ states of the compound and residual nuclei studied here. The number beside each level is the energy in MeV of that level above the ground state of the appropriate compound nucleus. The number in the lines connecting levels is the statistical factor for the isotopic spin change in that mode of decay. The displacement between the $T_>$ and $T_<$ states of a given nucleus was computed by the method of Jaffe and Harchol given in Ref. 35.

(ii) Varying the value of the pairing-energy parameter $\delta$ can give drastic changes in the relative probabilities for the emission of neutrons, protons, and $\alpha$ particles, but these relative probabilities will be essentially the same from corresponding entrance channels and thus cannot in themselves give rise to divergent ratios from corresponding entrance channels.

(iii) The introduction of an effective moment of inertia that is but a fraction of the rigid-body value enhances the probability of an $(\alpha, \alpha')$ reaction over that for the $(p, \alpha)$ and thus can qualitatively reproduce the divergences between the observed *ratios* of cross sections for corresponding reactions. The *cross sections* for the $(\alpha, \alpha')$ and $(p, \alpha)$ reactions, however, indicate that the probabilities of these two reactions should *not* be very different; rather, the divergence in the ratios is a consequence of an enhanced probability of the $(p, p')$ reaction over that of the $(\alpha, p)$. This latter effect does not appear as a consequence of varying the effective moment of inertia.

Thus, the observed divergences cannot be encompassed within the usual statistical theory including angular momentum conservation and odd-even effects. In the following section, the possibility of isotopic-spin conservation as a cause for the enhancement of the $(p, p')$ reaction will be considered.

### Isotopic-Spin Conservation

Yet to be explicitly included among the constants of the motion defined by the entrance channels is the isotopic spin. The observation of approximate isotopic spin conservation is well known in many systems varying over a wide range of $Z$ and $A$.[35] In this section, the consequences of the possible conservation of isotopic spin on nuclear reactions in the region of overlapping levels will be investigated.

Isotopic spin level schemes for the $Cu^{63}$ and the $Ni^{60}$ compound systems that are under investigation are presented in Fig. 16. It can be seen from these level schemes that while compound nuclei of but a single isotopic spin may be formed in $\alpha$-induced reactions, there are two possible states when protons are the bombarding particles. If we assume that the sticking probability is the same for forming both of these states, then their relative population is given by the square of the appropriate Clebsch-Gordan coefficients

$$\sigma(T_<, J, U/p) = [C_{tt'}(T_< T_z; t_z t_z')]^2 \sigma(J, U/p), \quad (6a)$$

$$\sigma(T_>, J, U/p) = [C_{tt'}(T_> T_z; t_z t_z')]^2 \sigma(J, U/p), \quad (6b)$$

[35] *Isotopic Spin in Nuclear Physics*, edited by J. D. Fox and D. Robson (Academic Press Inc., New York, 1966).

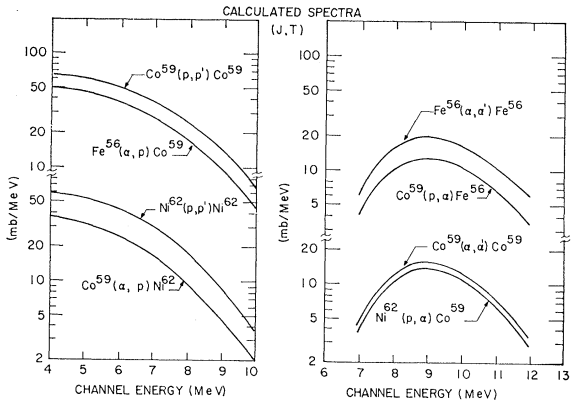


FIG. 17. Calculated proton and $\alpha$-particle energy spectra with both isotopic spin and angular momentum conserved.

where $t$ is the isotopic spin of the target, $t'$ is the isotopic spin of the incoming projectile, and $T_>$ and $T_<$ are the isotopic spins of the compound nucleus. For incident protons

$$t=t_z=(N-Z)/2=\text{ground-state isotopic spin of target}$$

$$t'\text{ (proton)}=\tfrac{1}{2},\qquad t_z'\text{ (proton)}=-\tfrac{1}{2},$$

$$T_<=t-\tfrac{1}{2},\qquad T_>=t+\tfrac{1}{2}.$$

In Eq. (6), it is assumed that, in a first approximation, the squares of the Clebsch-Gordan coefficients enter into the formation cross sections as weighting factors on the appropriate transmission coefficients $T_l(\epsilon)$. In contrast, when an $\alpha$ particle is used to form the compound nucleus, only one value of isotopic spin is possible because $t'=t_z'=0$. In essence, two distinct compound nuclei are formed with protons ($T=T_>$ and $T=T_<$) and one ($T=t$) with $\alpha$ particles. (Note that if $t$ is the isotopic spin of the target for incident protons, then the corresponding incident $\alpha$ channel must have a target of isotopic spin $t-\frac{1}{2}$.) Equation (1) should now be modified to read

$$\sigma(a,b)=\sum_{T,J}\sigma(T,J,U/a)W(b/T,J,U),\qquad(7)$$

where $T$ is the isotopic spin of the system and definition of the quantities $W$ and $\sigma$ are obvious extensions of those given in Eq. (1). Isotopic spin conservation appears explicitly in $W(b/T,J,U)$ in two ways:

(i) The transmission coefficients for the inverse of each exit channel must be weighted by the appropriate Clebsch-Gordan coefficients. For example, as may be seen from Fig. 16, the emission of protons from the $T=\frac{7}{2}$ state of $Cu^{63}$ to the $T=3$ state of $Ni^{62}$ entails a weighting factor of $\frac{1}{7}$, the emission of neutrons to the $T=2$ and $T=3$ states of $Cu^{62}$ are characterized by weighting factors of 0 and $\frac{6}{7}$, respectively.

(ii) The density of final states of the various residual nuclei must be that for the appropriate isotopic spin as well as the appropriate angular momentum and excitation energy. This effect was approximated in the present investigation by taking the level density of the excited isotopic spin states to be the same as that for the ground isotopic spin states of the isobaric-analog nucleus at the corresponding excitation energy. Thus, the level density of the $T=3$ states of $Cu^{62}$ at an excitation energy $U$, was taken to be the same as that for $Ni^{62}$ at an excitation energy of $U-\Delta$ where $\Delta$ is the usual isobaric-analog energy.[2,35] This means, of course, that there are no states of $T=3$ in $Cu^{62}$ for $U<\Delta$.

These two implications of isotopic spin conservation affect emission from $T_>$ and $T_<$ compound nuclei in different ways: Since the emission of any particle from the $T_<$ states can always go to states which are of the same isotopic spin as the ground state of the residual nucleus, the major effect will be that of weighting the competing exit channels by the appropriate Clebsch-Gordan coefficients. For the $T_>$ states, the emission of any particle that is not proton excess from a neutron excess compound nucleus can lead only to residual nuclei with isotopic spin at least one unit higher than that of the ground state of the residual nucleus. Thus, for example, the emission of a neutron from the $T=\frac{7}{2}$ state of $Cu^{63}$ cannot lead to the $T=2$ states of the residual $Cu^{62}$, but only to the $T=3$ and $T=4$ states. Since the level densities at a given excitation energy of these latter two states are much smaller than that for the ground isotopic spin state, the width for neutron emission is drastically reduced. Analogous constraints on $\alpha$-particle emission lead to similar results.

The conservation of isotopic spin thus suppresses neutron and $\alpha$ emission from $T_>$ compound nuclei (formed only with incident protons) and has but a small effect on the relative probabilities of the emission of particles from the $T_<$ compound nuclei (formed both with incident $\alpha$ particles and protons). Thus, the conservation of isotopic spin leads naturally to the result that $\sigma(p,p')/\sigma(p,\alpha)>\sigma(\alpha,p)/\sigma(\alpha,\alpha')$ for corresponding reactions while leaving the ratio $\sigma(p,\alpha)/\sigma(\alpha,\alpha')$ essentially the same as the ratio of the total reaction cross sections for protons and $\alpha$ particles in agreement with the experimental observations. The magnitude of the effect of isotopic spin conservation on the enhancement of the $(p,p')$ reaction depends on the values of the other parameters in the level-density expression. In particular, the effect will be largest if the parameters are such that the probability of proton emission from the $T_<$ compound nuclei is small.

An evaporation calculation was carried out for the $T_>$ states of the two compound systems by employing the energy displacements of the $T_>$ states of the residual nuclei with respect to their ground states (Fig. 16) and using the pairing energies of the appropriate analogs of the $T_>$ residual nuclei. In this calculation, the effective moments of inertia of the various nuclei involved were given the rigid-body value for a uniform sphere of radius $r_0A^{1/3}\times10^{-13}$ cm and the pairing energies $\delta$ were chosen so as to conform

to the experimental values for the $Co^{59}(\alpha, p)Ni^{62}$ (5–8 MeV) and the $Fe^{56}(\alpha, \alpha')Fe^{56}$ (7–12 MeV) cross sections.

It is to be noted that these latter two reactions do *not* entail emission from the $T_>$ states. The values of $\delta$ that are required are 3.11 MeV for $Ni^{62}$ and 3.25 MeV for $Fe^{56}$. The calculation shows, as expected, that neutron and $\alpha$ particle emission are almost completely inhibited from these $T_>$ states and that the proton spectra are essentially unchanged in shape from those calculated for the $T_<$ compound systems.

The calculated values of the previously mentioned ratio of cross sections given by the appropriate combinations of calculated spectra from the $T_>$ and the $T_<$ states are presented in Table VI along with the experimental values; the calculated spectra are exhibited in Fig. 17. Qualitatively, the inclusion of isotopic spin conservation moves the calculated results in the proper direction; a substantial enhancement of the cross section for the $(p, p')$ reaction along with relatively minor changes in those for the $(p, \alpha)$, $(\alpha, p)$, and $(\alpha, \alpha')$ reactions. No effort was made to achieve better quantitative agreement between calculated and experimental results by varying the parameters $\alpha$, $\delta$, and $I$. We wished only to show that isotopic spin is the sole possible constant of the motion that can remove the apparent violations of the independence hypothesis, other than shapes of corresponding spectra, that were observed in this experiment.

It is, of course, always possible to ascribe any unexpectedly large $(p, p')$ cross section to some direct process. Such a process may well, as a matter of fact, be involved in the emission of protons with channel energies in excess of 8 or 9 MeV. However, both the shapes and the angular distributions of those parts of the proton spectra that were analyzed here suggest that all possible interpretations within the context of the statistical model should be explored before invoking, for example, something like precompound decay[36] or other nonstatistical processes. On the other hand, the latter possibility cannot yet be excluded and further experiments are planned in an effort to clarify this point.

[36] J. J. Griffin, Phys. Rev. Letters **17**, 478 (1966); G. D. Harp, J. M. Miller and B. J. Berne, *ibid.* **165**, 1166 (1968); M. Blann, *ibid.* **21**, 1357 (1968).

## SUMMARY AND CONCLUSIONS

The experimental results on the two corresponding systems that have been investigated show that although the particle spectra that were observed in the backward direction have the characteristics expected for compound-nuclear reactions, both the ratios of cross sections of distinguishable exit channels and the shapes of particle spectra for corresponding reactions are different for different entrance channels. These differences are qualitatively consistent with the calculated divergences from the independence hypothesis that are expected from the possible effects of differing angular momentum and isotopic spin distributions in the corresponding entrance channels.

The requirement of angular momentum conservation int the calculations provides a qualitative understanding of the differences in the shapes of corresponding proton and $\alpha$ spectra; that is, the $(p, p')$ spectrum versus the $(\alpha, p)$ spectrum, and the $(\alpha, \alpha')$ spectrum versus the $(p, \alpha)$ spectrum. The difference in the observed ratio of cross sections, $\sigma(\alpha, p)/\sigma(\alpha, \alpha')$ and $\sigma(p, p')/\sigma(p, \alpha)$, are not, however, accounted for.

The inclusion of isotopic spin as well as angular momentum conservation in the calculations indicates the importance of its possible conservation on the ratio of cross-sections for distinguishable exit channels. The effects of isotopic spin conservation on these ratios are greatest when the $T_>$ state can be populated in the compound nucleus as occurs in the proton entrance channels, and are of the proper magnitude to explain the observed difference in the ratios of cross sections $\sigma(p, p')/\sigma(p, \alpha)$ and $\sigma(\alpha, p)/\sigma(\alpha, \alpha')$.

## ACKNOWLEDGMENTS

We wish to express our deep appreciation to Professor Ivor Preiss for his guidance and counsel during our runs at the heavy-ion accelerator at Yale. We are indebted to the operating crews of the Yale heavy-ion accelerator and the Columbia 37-in. cyclotron for their help and advice during the irradiations. Finally, we wish to thank Professor George Temmer for letting us do some runs on the Rutgers tandem accelerator and express our appreciation to both him and his coworkers for their kindness and help during our visits to Rutgers.